AIMS Materials Science, 7(4): 441–452.
DOI: 10.3934/matersci.2020.4.441
Received: 21 April 2020
Accepted: 16 June 2020
Published: 23 July 2020

http://www.aimspress.com/journal/Materials

Research article

Improving the structural properties and corrosion behaviour of electroless deposited Ni–P–Zn coatings on mild steel for advanced processes

Ojo Sunday Isaac Fayomi[1,3,*], Adedamola Sode[1], Itopa Godwin Akande[2], Abimbola Patricia Idowu Popoola[3] and Oluranti Agboola[4]

[1] Department of Mechanical Engineering, Covenant University, P.M.B 1023, Ota, Nigeria
[2] Department of Mechanical Engineering, University of Ibadan, Ibadan, Oyo state, Nigeria
[3] Department of Chemical, Metallurgical and Materials Engineering, Tshwane University of Technology, P.M.B. X680, Pretoria, South Africa
[4] Department of Chemical Engineering, Covenant University, P.M.B 1023, Ota, Nigeria

* **Correspondence:** Email: Ojosundayfayomi3@gmail.com; Tel: +2348036886783.

Abstract: Hydrated crystal of $ZnSO_4 \cdot 7H_2O$ was co-deposited with $NiSO_4 \cdot 6H_2O$, and $NaH_2PO_2 \cdot H_2O$ processed electrolyte to develop a ternary phase electroless coating on mild steel for advanced application. The coating was produced in an aqueous nickel electrolyte solution with zinc at a temperature of 90 ^oC and varying time conditions between 20 and 50 min. The effects of the developed coatings on microstructure and physical properties were investigated using scanning electron microscopy (SEM), Energy dispersive spectroscopy (EDS), and optical microscopy. The corrosion characteristics of the coatings examined in 0.5 M H_2SO_4 and 3.5% NaCl were analyzed using linear potentiodynamic polarization technique. The microstructure revealed that the constituent deposited on the steel. A more uniformly distributed crystallite with minimal pores was observed at 20 min of Ni–P–Zn coating, while the tiniest film was observed at 50 min of the coating without crack. There was also a fully compact grain within the intermetallic matrix of the coating due to the synergetic effect of the electrolyte constituent with the strengthening phase of $Zn_7Ni_4P_2$, Zn_2Ni_5P, and Zn_3Ni. Corrosion study established that Ni–P–Zn exhibits significant corrosion resistance at the optimum time within the examined environments with little SO_4^{2-} and Cl^- ions.

Keywords: microstructure; electroless; coating; corrosion; application

1. Introduction

Steel and their alloys are widely used materials in the world today and can be found in various industries such as production, chemical and electrochemical, transportation, construction, medicine and other industries [1–3]. The problems associated with most steel are their inability to resist corrosion because of their latent physical properties that provoke chemical ionic interaction and reactivity [4]. Curtailing corrosion occurrences with proper materials selection, equipment design, cathodic protection and through inhibition has been a proactive measure taken by several researchers in the field of surface science [5–7].

The alternative to the earlier mention methods is the use of coatings technologies to enhance and provide a suitable protective barrier on the steel [8]. Research and development in coatings have been massive over two decades ranging from single phase coating to binary and recently to ternary co-deposition in a single bath framework [9–11]. Deposition involves two major processes that have proved their usefulness in manufacturing application for decades. They are electroless and electrodeposition technology [12]. The electroless coating has undoubtedly given room for tremendous accomplishments in the field of hard surface coatings, due to its improved chemical and mechanical properties, such as corrosion mitigation, low coefficient of friction and many more [12–15]. Electrodeposition, on the other hand, is the more popular of the two, due to its ability to satisfy functional and decorative applications [16]. Although the electrodeposition process has a larger market for coating objects and precious items; the two deposition methods are chemical and electrochemical method, which is always used to provide a solution to the challenges of material deterioration putting into consideration the nature of the material, the corrosive medium and area of material application [17–20].

Recently, interest in the Ni–P coatings with crystallite of metals, salt, ceramics and oxides has been in use, as improvements for single nickel coatings on steel [21]. Besides, this second phase particle, it provides a novel dispersion and strengthening influence, promote good wear, high coating stability, promotes corrosion resistance and self-healing characteristics [22]. Today, despite the development of the novel system of coating for greater performance, the major setback has been the influence of process parameters on electroless coating performance and the metal. Generally, the deposition bath contains several processing bath agent and parameters that could influence surface modification. These parameters are the nature of bath constituent, temperature, rate of dispersion, stirring rate, and time function, etc. The literature shows that little study has been done on the electroless deposition of hydrated zinc crystallite under higher varying time effect [23]. Thus, this current study, attempt to evaluate the structural and corrosion properties of Ni–P–Zn coating with the effect of zinc crystal and time-varying effect on the developed coating for the advance application. The introduction of zinc is as a result of it anti-corrosion ability. Zinc is known to be more reactive than mild steel, thus will be able to attract almost all local oxidation and also improve mechanical properties of mild steel [24,25]. Therefore, it was proposed that the synergy between the nanoparticles from Ni–P and Zn will largely.

2. Experimental methods

2.1. Sample preparation

The mild steel plate used in the study was sectioned into a rectangular shape of 40 mm × 40 mm × 2 mm with the help of struers discontom precision cutter at 600 rpm. The steel plate purchased from a metal processing vendor in Ota, Nigeria, was analyzed accordingly. The percentage nominal weight composition of the mild steel substrate is presented in Table 1. The corrosion propagation was done using AUTO LAB PGSTAT 101 potentiostat galvanostat device with Nova 2.1 software. The structural properties of the starting materials were analyzed using a scanning electron microscope equipped with an energy dispersive spectrometer. All chemical reagents used are Analar grade and conformed to standard for electroless setup. The bath formulation was prepared a day to the deposition proper for even dispersion in line with the study by [5].

Table 1. Compositional value in weight percent of un-plated mild steel.

Element	S	Mn	Si	Ni	Al	P	C	Fe
Composition (%)	0.02	0.15	0.016	0.01	0.01	0.01	0.032	Balance

2.2. Electroless bath and formulation

All chemical used in this study was obtained and supplied to Surface Engineering Research Laboratory, Covenant University from Sigma-Aldrich, USA. $NiSO_4 \cdot 6H_2O$, $ZnSO_4 \cdot 7H_2O$, and $NaH_2PO_2 \cdot H_2O$ salt were obtained in powder nature. $NiSO_4 \cdot 6H_2O$, which is the based salt, has a density of 2.07 g/cm^3, solubility in water of 77.5 g/mL at 30 ^oC. $ZnSO_4 \cdot 7H_2O$ is a hydrated crystal that crystallizes in orthorhombic nature with a density of 3.31 g/cm^3 dissolve freely in the water at 280 ^oC and molar mass of 287.54. The weight percentage of the $ZnSO_4 \cdot 7H_2O$ is at a constant concentration of 5 g/L. The bath formulation was obtained by dissolving in 1 litre of deionized water 30 g of $NiSO_4 \cdot 6H_2O$, 5 g of $ZnSO_4 \cdot 7H_2O$, 33 g of $NaH_2PO_2 \cdot H_2O$, 60 g of $C_6H_5 \cdot Na_3O_7 \cdot 2H_2O$, 25 g of $(NH_4)_2SO_4$, 10g of H_3BO_3, 10g of Thiourea at pH of 5. The bath was allowed to dissolve appropriately after leaving it for 24 h. Most of the admixtures constituting the bath formulation are for quick conductivity of cation, brightener, buffers, and refiners.

2.3. Electroless set-up

By using autocatalysis process, the bath is put into a non-reactive container with 500 mL, a conical flask made from glass, and placed on a hot stirrer. The contents of the bath are heated to a temperature range of 85 ± 50 ^oC with the help of a metal bulb thermometer. The mild steel samples were suspended by a simple beam structure into the heated compound, and given sufficient time to develop a thin film layer. Each sequential coating deposition was done for an uninterrupted time up to 50 min at a stirring rate of 250 rpm to ensure uniformity of coating. The components of the bath were changed after each time cycle of 20 min, 30 min, 40 min and 50 min respectively in the presence of 5 g/L of $ZnSO_4 \cdot 7H_2O$. After each experimental process, according to deign in Table 2, the samples were air-dried and stored in a cool and dry place.

Table 2. Experimental design of study.

Sample coating	Time (min)
Ni–P–Zn	20
Ni–P–Zn	30
Ni–P–Zn	40
Ni–P–Zn	50

2.4. Analysis of electroless deposited samples

The microstructure properties of the developed electroless nickel-phosphate and nickel-phosphate induced composite additive were examined using a High tech optical microscope, scanning electron microscope (SEM and energy dispersive spectroscopy (EDS). The VEGA 3, TESCAN model SEM function by examining surface morphology and crystal orientation. The X-ray diffraction study was carried out using X'Pert Pro model diffractometer to pattern the phases present on the resulting deposits. A Cu Kα source on the X'Pert Pro model diffractometer set at 40 kV was used to scan in range between 10^o and 90^o two theta (2θ). The coating thickness was analysed using Positector 6000IP micro-thickness meter for dry film thickness.

2.5. Corrosion analysis

Study of the corrosion properties of all developed coating was examined using the potentiodynamic polarization technique. The produced coating samples were subjected to 0.5 M H_2SO_4 and 3.5% NaCl environments at an ambient temperature of (27 ± 1 ^{o}C). A three conventional electrode cell consisting of the reference electrode, working electrode, and counter electrode with a beaker filled with 100 mL of electrolyte was used. With the mild steel as the working electrode, silver chloride as the reference electrode, and graphite rod as the counter electrode, the configuration was connected to AUTO LAB PGSTAT 101 Metrohm. The Tafel plot was attained within −1.5 V and +1.5 V and a scan rate of 0.0012 V/s which is in line with the study by [8] at several concentrations and while changing the temperature of the system.

$$IE\ (\%)\ =\ \frac{(Jcorr)a-(Jcorr)p}{(Jcorr)a}\ \times\ 100 \tag{1}$$

where (*Jcorr*)*a* and (*Jcorr*)*p* represent the corrosion density (A/cm^2) in the absence and presence of the particulate, respectively.

The corrosion rate (CR) is determined using the Eq 2:

$$CR\ (mm/yr)\ =\ \frac{0.00327 \times J_{CORR} \times E_w}{D} \tag{2}$$

where J_{CORR} is the current density in μA/cm^2, D is the density of copper g/cm^3 (8.96 g/cm^3), E_w is the equivalent weight in gram of mild steel.

3. Results and discussion

Table 3 is the relationship between the change in time of deposition and the coating matrix with interest on physical characteristics. The properties of developed coating in term of weight gain and coating per unit area as the time increase is shown in Table 3 as well. It can be seen that the weight gain of the NiP–Zn-50 min electroless deposited coating increased with increase in time with 0.0981 g to 0.030656 A/m^2 for weight gained and coating per unit area respectively. The lowest in the pattern is the coating at Ni–P–Zn-20 min with 0.0561 g to 0.017531 A/m^2 respectively. All developed coating possesses excellent weight and coverage in response to time trend. One can certainly established that deposition parameter with time consideration influence the pattern of coating geometry before possible agglomeration could form. Also, the description on the coating matrix denote that coating time is directly proportional to the coating thickness, or amount of deposition as shown in Table 3. We also note that there is correlation between the electroless process parameter and coating thickness. An increase in time influences the increases in the coating thickness evolution from 18.25 to 20.54 μm. Though in reported study by [4], there is linear relationship between time of coating and coating amount deposited on substrate which influences structure and physical performance.

Table 3. Electroless parameters and results for Ni–P–Zn coating.

Sample coating	Time (min)	Weight gain (g)	Coating per unit area (mg/mm^2)	Coating thickness (μm)
NiP–Zn	20	0.0561	0.017531	18.25
NiP–Zn	30	0.0593	0.018531	18.29
NiP–Zn	40	0.0729	0.022781	18.95
NiP–Zn	50	0.0981	0.030656	20.54

Figure 1a–d shows the scanning electron microscope microstructure of the Ni–Zn–P samples under difference in time of deposition from 20, 30, 40 and 50 min respectively. The sample images were taken at 1000× magnification, with acceleration voltage of 20 kV, working distance 50 μm. Figure 1a shows the gradual growth in deposits and crystals occurring from the nickel and zinc particles in the presence of phosphate salt [2–5]. The effect of time was appreciated with beneficial crystal evolution diffused and properly controls by the bath contents. A significant hard coating was seen with amorphous structure but with boundaries distortion and unstable flakes film deposited in Figure 1b when time was increased to 30 min. The grain growth was more distinctive with hexagonal layer in larger form uniformly distributed at the lattice but with short boundaries fusing the coating together. With careful look at the deposited coating in 30 min, there seem to be development of pores and smaller micro-crack with Zn ion could not properly adsorbed as desire, which is in line with study by [23] especially with lower time of coating. Interestingly, film formation was seen to completely change for 40 min deposit with zinc ion rapid precipitation and substitution at the atomic radial of Ni–P pores dramatically begins to create new surface modification. It is evident that time influence changes the coating mechanism and at the same time deepens the nature of coating deposited. In an attempt to increase coating compactness', deposition time was increase to 50 min and the microstructural evolution takes a different pattern with better order crystallinity and sharp reduction in residual stress. There is an excellent crystal formation and smaller grain size attributed

to interfacial responses of the bath and time effect. The growth was evenly achieved and well dispersed on the mild steel substrate with homogenously bounded nucleation without pores and cracks at the active sites of the steel (see Figure 1d). More so, this result also acknowledged the fact that that time variable parameter provides effective change in coating thickness progression which influence the structural crystal orientation and bounding activities of the developed coatings.

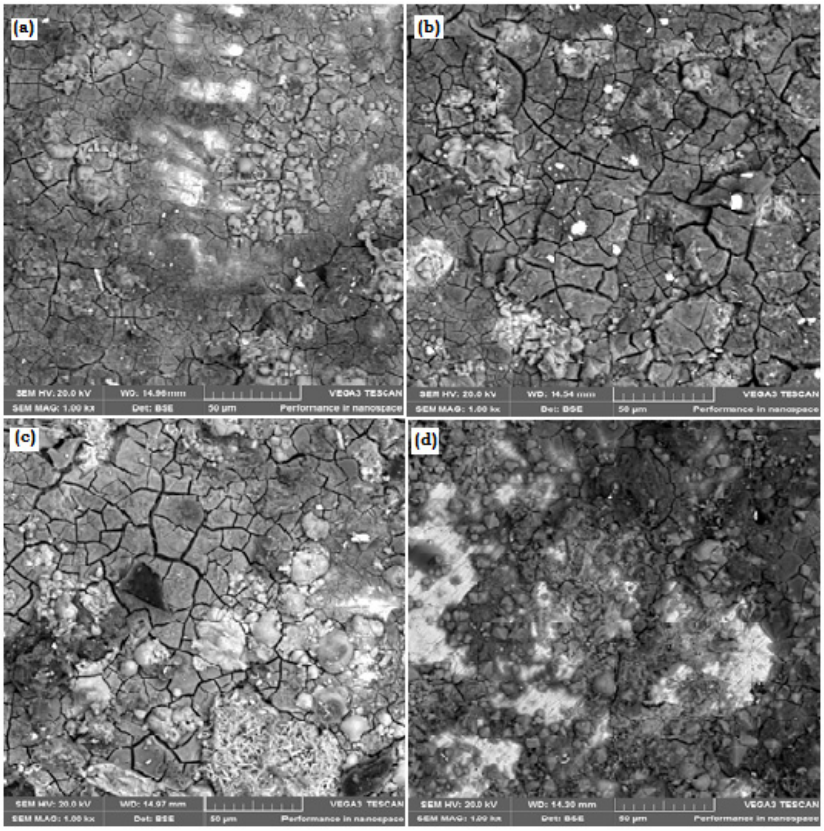

Figure 1. SEM crystal evolution of electroless codeposition of Ni–P–Zn mild steel surface at 1000× magnification (a) 20, (b) 30, (c) 40, and (d) 50 min.

Figure 2 shows the EDS elemental composition of the Ni–Zn–P coating at 50 min with the presence of major particle constituent like zinc, nickel and phosphorus with weight deposit of 22.1 wt%, 6.8 wt% and 15.6 wt% respectively. Zinc and oxygen have a dominate interfacial bonding weight presence with peak pattern showing dispersive distribution of the particulates on the mild steel surface. It can be conclude that zinc crystals retain its ions species on nickel and phosphorus growth and prominently take a wider surface area on the steel surface.

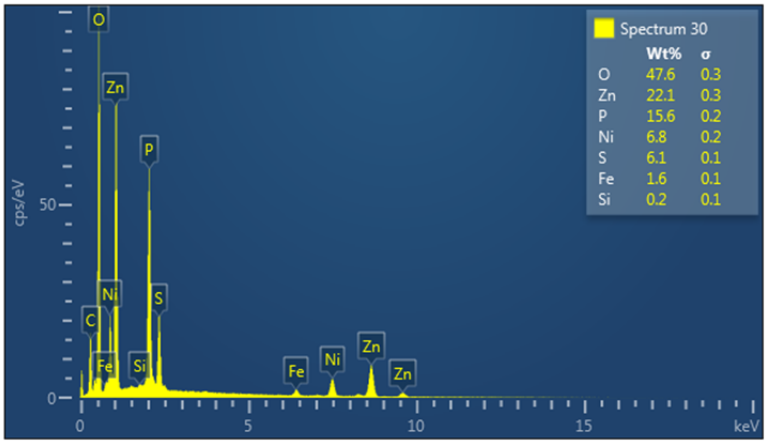

Figure 2. EDS of Ni–P–Zn electroless deposited mild steel surface at 50 min.

The effect of deposition time on the intermetallic phase propagation of Ni–P–Zn deposition in 50 min is shown in Figure 3. We observed that there is a unique correlation between the morphology and phase composition. At higher time influence, solid crystal structure within Ni matrix becomes amorphous without permitting crack evolution [12]. It is worthy to mention, that phase crystallinity within the interfacial structure increases due to integration of Zn into the Ni Fcc alloy phase, thus promoting resistance hybrid against crack. The corrosion resistance properties of electroless deposited alloy are presented in Figures 4 and 5 indicating the potentiodynamic polarization and open circuit potential trends. The influence of potential-current deviation was examined in 0.5 M H_2SO_4 for all coating matrix. From the obtained result in Table 4, the deposition of the electroless deposited coating of Ni–P–Zn alloy for 40 and 50 min generally show passive surface protection. The corrosion rate decrease with increase in deposition time. Meanwhile, the Ni–P–Zn-20 min coated mild steel shows polarization resistance of 76.232 Ω, corrosion rate of 3.46486 mm/yr and corrosion potential effect of −0.7210 V. At NiP–Zn-50 min, strong load bearing and resilient crystal formation was seen to provide decrease in degradation trend with polarization resistance of 120.12 Ω, corrosion rate of 1.1210 mm/yr, and corrosion potential of −0.6998 V. The corrosion properties demonstrated contention of diffused particle retarding severity of SO_4^{2-} species and intermolecular ions [6]. It is worth mentioning that strong coating adhesion, contribute to the retarding ions which ought to cause crevices and pit formation.

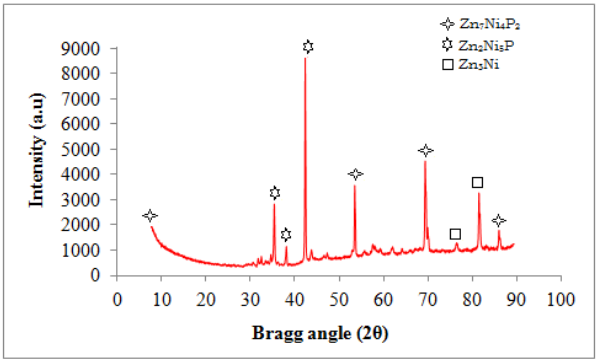

Figure 3. XRD of Ni–P–Zn electroless deposited mild steel surface at 50 min.

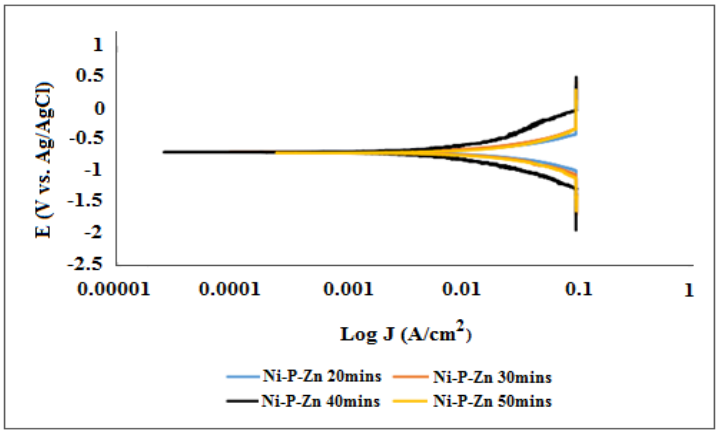

Figure 4. Potentiodynamic polarization curve for electroless deposited Ni–P–Zn at various time interval, in 0.5 M H_2SO_4.

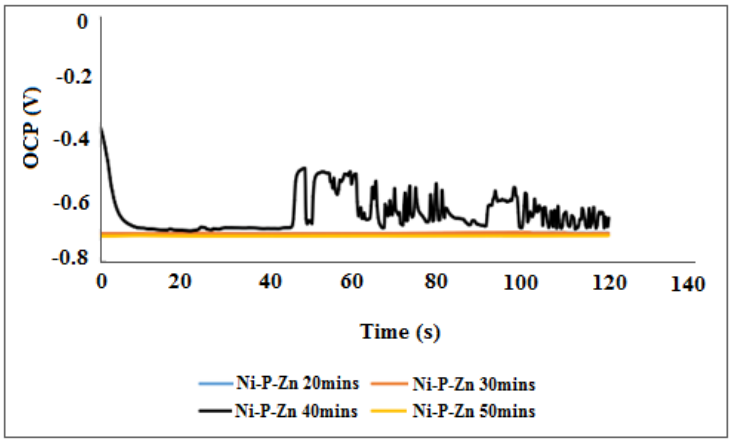

Figure 5. Open circuit potential curve for electroless deposited Ni–P–Zn at various time interval, in 0.5 M H_2SO_4.

Table 4. Potentiodynamic polarization table for electroless deposited Ni–P–Zn at various time interval, in 0.5 M H_2SO_4.

Sample label	Ecorr (V)	Jcorr (A/cm^2)	Corrosion rate (mm/yr)	Polarization resistance (Ω)
NiP–Zn-20 min	−0.7210	0.0029005	3.6486	76.232
NiP–Zn-30 min	−0.7170	0.0028878	1.4036	100.54
NiP–Zn-40 min	−0.7100	0.0023802	1.4138	115.54
NiP–Zn-50 min	−0.6998	0.0023335	1.1210	120.12

The susceptibility of the electroless deposited coatings in 3.65% NaCl solution is presented in Figures 6 and 7. Table 5 also show the Tafel extrapolation data with time function. Though, similar trend was notice as the induced corrosion propagation of 0.5 M H_2SO_4 series. Chloride penetration was massive compare to sulphate ion. Ni–P–Zn-50 min has polarization resistance of 78.000 Ω, corrosion rate of 1.9211 mm/yr and corrosion potential effect of −1.7210 V. The lower corrosion properties with lower coating deposited with low time of deposition of 61.361 Ω, corrosion rate

of 4.2100 mm/yr and corrosion potential effect of −1.2110 V. This observation implies that there is Fe^{2+} reduction as a result of Cl evolution and redox mechanism which prompt quick dissolution of crystal coatings.

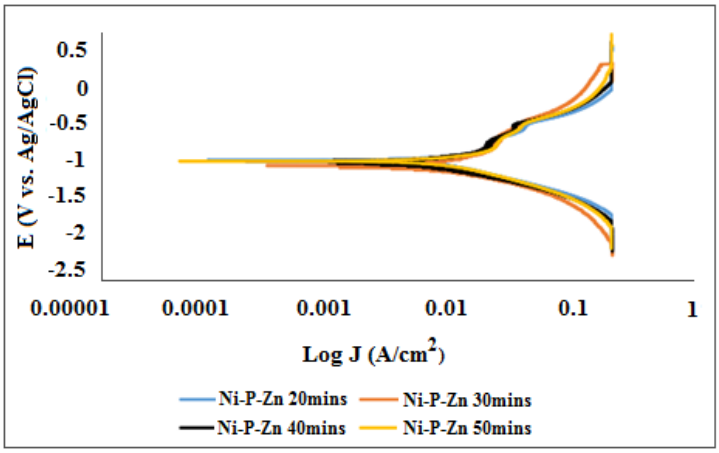

Figure 6. Potentiodynamic polarization curve for electroless deposited Ni–P–Zn at various time interval in 3.5% NaCl.

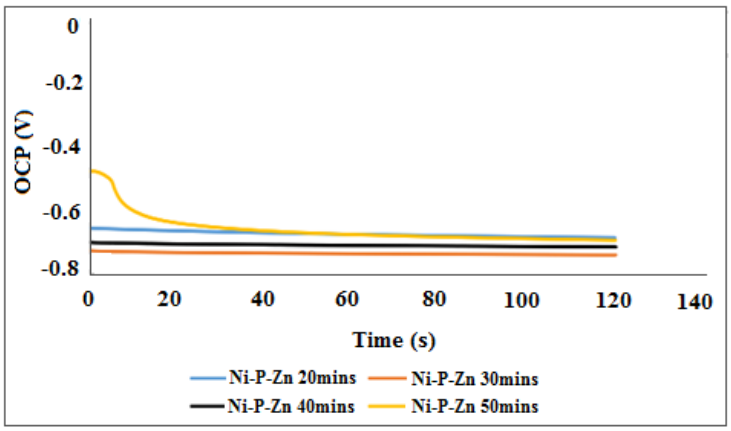

Figure 7. Open circuit potential curve for electroless deposited Ni–P–Zn at various time interval in 3.5% NaCl.

Table 5. Potentiodynamic polarization table for electroless deposited Ni–P–Zn at various time interval in 3.5% NaCl.

Sample label	Ecorr (V)	Jcorr (A/cm^2)	Corrosion rate (mm/yr)	Polarization resistance (Ω)
NiP–Zn-20 min	−1.2110	0.009800	4.2100	61.361
NiP–Zn-30 min	−1.2100	0.009720	4.2001	62.231
NiP–Zn-40 min	−1.1201	0.009101	1.8672	72.321
NiP–Zn-50 min	−1.1001	0.008999	1.9211	78.000

Figure 8 shows the corroded micrograph of the electroless deposited coating in its varied time effect. Pitting evolution was seen to be more with scale fall out like corrosion product in NiP–

Zn-20 min as seen in Figure 8a. The change in the degradation is due to the chloride adsorption in the metal ion and influence of process parameter, though, agglomerated deposits on mild steel coated surface was seen to scuff out at the coating interface. In Figure 8b–d, all coated alloy maintain their coating stability with passive character. It can be concluded that zinc addition causes perfect nucleation for NiP matrix which absolutely promote effective stabilization of active passive behaviour of coated mild steel against pit occurrences.

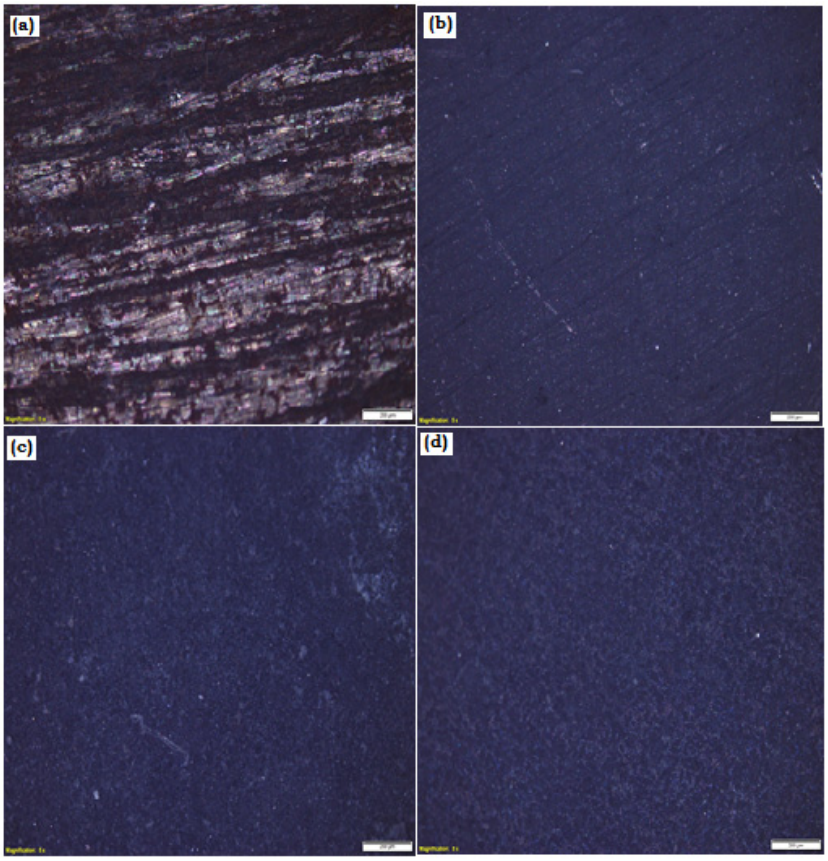

Figure 8. Micrograph of corroded Ni–P–Zn deposited on mild steel surface at 5× magnification (a) 20 min (b) 30 min (c) 40 min and (d) 50 min in 3.5% NaCl.

4. Conclusion

It is realistic to produce Ni–P coating with electroless deposition route with addition of hydrated crystal of $ZnSO_4 \cdot 7H_2O$ to provide solid crystal nucleation and passive stable coating. The polarization potential of all the fabricated coatings of Ni–P–Zn matrix increase as the time of deposition increases. The highest corrosion resistance was obtained at 50 min deposition with 120.12 Ω, which represents over 50% increase of the coating deposited at 20 min. The degradation trend after coating was minimal due to mixed character of the developed matrix and their heter-atoms active participation. Notably, the $ZnSO_4 \cdot 7H_2O$ incorporation in the electroless plating bath gives a new narratives in the morphology and the elemental composition of the developed alloys.

Acknowledgements

The authors appreciate gracefully the financial support of Covenant University and Surface Engineering Research Laboratory, Department of Mechanical Engineering, Covenant University for equipment usage.

Conflict of interests

The authors will like to declare that this research has no any financial or work related competing interest.

References

1. Anawe PAL, Fayomi OSI, Popoola API (2017) Results in physics investigation of microstructural and physical characteristics of nano composite tin oxide-doped Al^{3+} in Zn^{2+} based composite coating by DAECD technique. *Results Phys* 7: 777–788.
2. Dai J, Liu X, Zhai H, et al. (2009) Preparation of Ni-coated Si_3N_4 powders via electroless plating method. *Ceram Int* 35: 3407–3410.
3. Du N, Pritzker M (2003) Investigation of electroless plating of Ni–W–P alloy films. *J Appl Electrochem* 33: 1001–1009.
4. Dai J, Liu X, Zhai H, et al. (2009) Preparation of Ni-coated Si_3N_4 powders via electroless plating method. *Ceram Int* 35: 3407–3410.
5. Aydoğdu GH, Aydinol MK (2006) Determination of susceptibility to intergranular corrosion and electrochemical reactivation behaviour of AISI 316L type stainless steel. *Corros Sci* 48: 3565–3583.
6. Ayoola AA, Fayomi OSI, Ogunkanmbi SO (2018) Data in brief data on inhibitive performance of chloraphenicol drug on A315 mild steel in acidic medium. *Data in Brief* 19: 804–809.
7. OO A, Nwaokocha C, Adesanya A (2012) Evaluation of corrosion cost of crude oil processing industry. *JESTEC* 7: 517–518.
8. Amin MM, Kee LK, Yunus K (2002) The process of electroplating in the presence of nickel salts. *Ultra Sci* 14: 309–318.
9. Ehteram A, Aish H (2008) Corrosion behavior of mild steel in hydrochloric acid solutions. *Int J Electrochem Sci* 3: 806–818.
10. Equbal A, Dixit NK, Sood AK (2013) Electroless plating on plastic. *IJSER* 8: 12–18.
11. Gao W, Cao D, Jin Y, et al. (2018) Microstructure and properties of Cu–Sn–Zn–TiO_2 nano-composite coatings on mild steel. *Surf Coat Tech* 350: 801–806.
12. Guo D, Zhang M, Jin Z, et al. (2006) Pulse plating of copper-ZrB_2 composite coatings. *J Mater Sci Technol* 22: 514–518.
13. House K, Sernetz F, Dymock D, et al. (2008) Corrosion of orthodontic appliances—should we care? *Am J Orthod Dentofac* 133: 584–592.
14. Kallappa D, Venkatarangaiah VT (2018) Synthesis of CeO_2 doped ZnO nanoparticles and their application in Zn-composite coating on mild steel. *Arab J Chem* 3: 45–60.
15. Krishnan KH, John S, Srinivasan KN, et al. (2006) An overall aspect of electroless Ni–P depositions—A review article. *Metall Mater Trans A* 37: 1917–1926.

16. Balaraju JN, Narayanan TS, Seshadri SK (2003) Electroless Ni–P composite coatings. *J Appl Electrochem* 33: 807–816.
17. Agarwala RC, Agarwala V (2003) Electroless alloy/composite coatings: A review. *Sadhana-Acad P Eng S* 28: 475–493.
18. Kumar S, Pande S, Verma P (2015) Factor effecting electro-deposition process. *IJCET* 5: 700–703.
19. Laudisio G, Seipel B, Ruffini A, et al. (2005) Corrosion behavior of Si_3N_4–TiN composite in sulphuric acid. *Corros Sci* 47: 1666–1677.
20. Pang JN, Jiang SW, Lin H, et al. (2016) Significance of sensitization process in electroless deposition of Ni on nanosized Al_2O_3 powders. *Ceram Int* 42: 4491–4497.
21. Popoola API, Fayomi OSI (2016) Effect of some process variables on zinc coated low carbon steel substrates. *Sci Res Essays* 6: 4264–4272.
22. Zarras P, Stenger-Smith JD (2014) Corrosion processes and strategies for prevention: An introduction, In: Makhlouf ASH, *Handbook of Smart Coatings for Materials Protection*, Woodhead Publishing 64: 3–28.
23. Akande IG, Oluwole OO, Fayomi OSI (2018) Optimizing the defensive characteristics of mild steel via the electrodeposition of Zn–Si_3N_4 reinforcing particles. *Def Technol* 14: 1–7.
24. Liu Y, Zhou X, Lyon SB, et al. (2017) An organic coating pigmented with strontium aluminium polyphosphate for corrosion protection of zinc alloy coated steel. *Prog Org Coat* 102: 29–36.
25. Ge T, Zhao W, Wu X, et al. (2020) Incorporation of electro conductive carbon fibers to achieve enhanced anti-corrosion performance of zinc rich coatings. *J Colloid Interf Sci* 567: 113–125.

AIMS Press